

1 'Candidatus Tisiphia' is a widespread
2 Rickettsiaceae symbiont in the mosquito
3 *Anopheles plumbeus* (Diptera: Culicidae)

4 **Authors**

5 Helen R. Davison¹, Jessica Crozier¹, Stacy Pirro², Doreen Werner³, Gregory D.D. Hurst¹

6 **Affiliations**

7 1. Institute of Infection, Veterinary and Ecological Sciences, University of Liverpool,
8 Crown Street Liverpool L69 7ZB UK
9 2. Iridian Genomes, Bethesda, MD, USA
10 3. Leibniz Centre for Agricultural Landscape Research (ZALF), 15374 Müncheberg,
11 Germany

12 **Corresponding Author**

13 Helen R. Davison - hlhdavi5@liverpool.ac.uk

14 **Author contributions**

15 Conceptualisation, supervision, methodology and funding acquisition – HRD and GDDH
16 Resources – HRD, DW, and SP
17 Investigation – JC and HRD
18 Analysis, Visualisation, and Data Curation – HRD
19 Original Draft Preparation – HRD, GDDH

20 **Data availability statement**

21 Genome bioproject accessions: PRJNA694375 and PRJNA901697. PCR sequences are
22 deposited in accessions OQ512853-OQ512860
23 Supplementary data is available online at: <https://doi.org/10.6084/m9.figshare.21865416.v1>

24 **Acknowledgments**

25 **Funding statement**

26 NERC ACCE Doctoral Training Studentship NE/L002450/1

27 Genome sequencing was supported by Iridian Genomes, grant# IRGEN_RG_2021-1345

28 Genomic Studies of Eukaryotic Taxa

29 **Ethical approval statement**

30 All samples were collected in accordance with ethical standards for insect collection.

31 **Conflicts of interest**

32 The authors declare no conflicts of interest.

33 **Abstract**

34 Symbiotic bacteria alter host biology in numerous ways, including the ability to reproduce or
35 vector disease. Deployment of symbiont control of vector borne disease has focused on
36 *Wolbachia* interactions with *Aedes* and is hampered in *Anopheles* by a lack of compatible
37 symbioses. Previous screening found the symbiont 'Ca. Tisiphia' in *Anopheles plumbeus*, an
38 aggressive biter and potential secondary vector of malaria parasites and West Nile virus. We
39 screen *An. plumbeus* samples collected over a ten-year period across Germany and use
40 climate databases to assess environmental influence on incidence. We find a 95% infection
41 rate that does not fluctuate with broad environmental factors. Microscopy suggests the
42 infection is maternally inherited based on strong localisation throughout the ovaries. Finally,
43 we assemble a high-quality draft genome of 'Ca. Tisiphia' to explore its phylogeny and
44 potential metabolism. This strain is closely related to those found in *Culicoides* midges and
45 shows similar patterns of metabolic potential. *An. plumbeus* provides a viable avenue of
46 symbiosis research in anopheline mosquitoes, which to date have one other proven
47 infection of a heritable symbiont. Additionally, it provides future opportunity to study the
48 impacts of 'Ca. Tisiphia' on natural and transinfected hosts, especially in relation to
49 reproductive fitness and vector efficiency.

50 Introduction

51 Bacterial symbionts in insects form vital components of their host's biology, ecology, and
52 evolution. They are known to influence how insects reproduce, how they respond to
53 environmental stress, and they interact with pathogens (Dunbar *et al.*, 2007; Himler *et al.*,
54 2011; Vega, Arribére and Castro-Vazquez, 2012; Hendry, Hunter and Baltrus, 2014; Xie *et al.*,
55 2014; Hayashi *et al.*, 2016). Several species of symbionts are vertically inherited from one
56 generation to the next, usually through the maternal germline, and may become intrinsically
57 linked with their host physiology, metabolism, and development (Buchner, 1965; Zchori-Fein,
58 Borad and Harari, 2006; Moran, McCutcheon and Nakabachi, 2008; Kremer *et al.*, 2009;
59 Giorgini *et al.*, 2010). Most importantly, symbionts have been deployed in the control of
60 vector populations and vector competence (Hoffmann *et al.*, 2011).

61 Success in symbiont-mediated disease control has been restricted to species from the genus
62 *Aedes*. Transinfection with *Wolbachia* from a drosophilid fly has been successfully used to
63 alter vector competence and lower risk of catching dengue fever from *Aedes aegypti*
64 (Linnaeus, 1762) in endemic areas (Hoffmann *et al.*, 2011; Walker *et al.*, 2011; Pereira *et al.*,
65 2018). However, important vectors like *Anopheles* are rarely naturally infected with
66 *Wolbachia*, and species within the group are commonly unreceptive to artificial *Wolbachia*
67 infections (Hughes *et al.*, 2014). In *Anopheles* mosquitoes, for instance, there is a single well-
68 established case of natural *Wolbachia* infection (Walker *et al.*, 2021). Therefore, it is desirable
69 to find potential alternatives that are either more capable of surviving transinfection or alter
70 vector competence in the native host species.

71 We previously detected the symbiont 'Ca. Tisiphia' (= Torix group *Rickettsia*) in *Anopheles*
72 *plumbeus* (Stephens, 1828) in the UK (Pilgrim *et al.*, 2021). *An. plumbeus* is broadly distributed
73 across Europe and is an indiscriminate biter. It is also capable of transmitting West Nile virus
74 and malaria parasites, although these pathogens do not natively occur in the majority of the
75 mosquito species' known distribution range, and vector competence has only been tested in
76 the laboratory setting (Bueno-Marí and Jiménez-Peydró, 2011; Dekoninck *et al.*, 2011;
77 Schaffner *et al.*, 2012). It has been highlighted as a species that could act as a secondary vector
78 of "tropical" disease agents as changing climate causes their northward spread and their
79 associated primary hosts like *Aedes albopictus* (Skuse, 1894) (Schaffner *et al.*, 2012; Heym *et*
80 *al.*, 2017).

81 'Candidatus Tisiphia' (= Torix group *Rickettsia*) appear to be particularly associated with hosts
82 deriving from wet or aquatic environments and may originate from symbionts of freshwater
83 ciliates (Driscoll *et al.*, 2013; Schrallhammer *et al.*, 2013; Kang *et al.*, 2014). Infection with this
84 symbiont occur in a broad range of invertebrates, from annelids to gastropods to arthropods
85 (Pilgrim *et al.*, 2021), as well as in algae (Hollants *et al.*, 2013) and amoebae (Dyková *et al.*,
86 2013). Their relatives in *Rickettsia* are capable of nutritional symbioses, protecting against
87 fungal infections and reproductive manipulation (Hurst *et al.*, 1994; Giorgini *et al.*, 2010;
88 Hendry, Hunter and Baltrus, 2014; Bodnar *et al.*, 2018). However, the known effects of 'Ca.
89 Tisiphia' are limited to an association with increased host size in *Torix* leeches, and weak
90 impacts on fecundity in *Cimex lectularius* bedbugs (Kikuchi and Fukatsu, 2005; Thongprem *et*
91 *al.*, 2020). There is no observed congruence of host and symbiont phylogeny, indicating that
92 host shifts occur commonly and that long-standing associations with species are rare. External
93 influence such as temperature or natural enemies can also influence the prevalence of
94 symbionts in host populations (Cass *et al.*, 2016; Corbin *et al.*, 2017; Leclair *et al.*, 2017).

95 Here we use PCR assays to establish the extent of 'Ca. Tisiphia' infection in *An. plumbeus*
96 mosquitoes across Germany collected by DW and through citizen science initiatives, and
97 assess associations with temperature, precipitation, and forest type. We also sequence and
98 assemble a high-quality draft genome for the symbiont 'Ca. Tisiphia' and provide evidence of
99 vertical transmission of the symbiont through the maternal germline through FISH imaging.
100 The symbiont genome is examined through bioinformatics approaches to establish potential
101 nutritional or protective symbioses.

102 Experimental Procedures

103 Collection of *Anopheles plumbeus* (Stephens, 1828)

104 Two hundred and fifty five *An. plumbeus* specimens were collected from 2012-2021 across
105 Germany by DW and citizen volunteers as part of the mosquito atlas (Mückenatlas) project
106 (Werner *et al.*, 2014). These were stored in 70% ethanol or dry (see supplementary materials
107 for storage and exact geographic information). *Post hoc* analysis indicated storage method
108 did not affect detection of symbionts by PCR assay.

109 Specimens were also collected by HD as larvae and raised to adults in water collected from
110 their larval pools. These specimens were either killed by flash freezing in liquid nitrogen prior

111 to genomic DNA extraction, or in 4% paraformaldehyde solution prior for fluorescence
112 imaging.

113 **DNA extraction and PCR screening of *Anopheles plumbeus* for 'Ca. Tisiphia'**

114 Promega Wizard® Genomic DNA Purification kit was used for DNA preparation. DNA quality
115 was then checked with a combination of HCO/C1J primers HCO_2198 (5'-TAA ACT TCA GGG
116 TGA CCA AAA AAT CA-3')/CIJ_1718 (5'-GGA GGA TTT GGA AAT TGA TTA GT-3') (Folmer *et al.*,
117 1994; Hajibabaei *et al.*, 2005; Siozios *et al.*, 2020). *Ca. Tisiphia* presence was assessed with a
118 PCR assay amplifying the 320-bp region of the 17 kDa OMP gene Ri17kD_F (5'-
119 TCTGGCATGAATAAACAGG-3')/Ri17kD_R (5'-ACTCACGACAATATTGCC-3') (Pilgrim *et al.*,
120 2017). PCR conditions used were as follows: 95 °C for 5 min, followed by 35 cycles of
121 denaturation (94 °C, 30 s), annealing (54 °C, 30 s) and extension (72 °C, 120 s).

122 A selection of 'Ca. Tisiphia' amplicons from positive samples across time and space were
123 Sanger-sequenced through Eurofins barcode service and identity confirmed by comparing the
124 sequences to the NCBI database via BLAST homology searches. These sequences are
125 deposited in accessions OQ512853-OQ512860.

126 **Association of symbiont prevalence with geographic and climatic information**

127 Annual average monthly temperature and precipitation data were retrieved for each sample's
128 coordinate and year from TerraClim (Abatzoglou *et al.*, 2018) which has a spatial resolution
129 of ~4-km (1/24th degree). Forest cover data was retrieved from Copernicus land datasets for
130 2018 (European Union, 2018) and raster data for forest type extracted in QGIS 3.16 (QGIS.org,
131 2020) within a 3km radius of each sample location. *Anopheles plumbeus* has historically been
132 recorded to have a maximum flight range of up to 13km (Becker *et al.*, 2010). However, this
133 is based on one single study from 1925 and is not verified by other sources. As such we chose
134 an estimated range of 3km based on the average flight ranges other anopheline mosquito
135 species (Becker *et al.*, 2010; Verdonschot & Besse-Lototskaya, 2014). Scikitlearn's standard
136 scaler (Pedregosa *et al.*, 2011) was applied to data before performing a generalised linear
137 model with a binomial logit link function on data with the following formula:

138 *Infected* ~ *tasmin* + *tasmax* + *precip* + *forest_ratio*

139 All statistics and geographic inferences were carried out in Python with the packages
140 Statsmodel and Scikit-learn (Rossum and Drake, 2009; Seabold and Perktold, 2010; Pedregosa

141 *et al.*, 2011). QGIS 3.16 was used to produce maps and extract raster data for forest types
142 before passing it to Python for analysis (QGIS.org, 2020). All other figures were produced with
143 Matplotlib and Seaborn (Hunter, 2007; Waskom and Seaborn development team, 2020).

144 **Fluorescence in situ microscopy (FISH)**

145 Reproductive organs of a single female and a single male were dissected and incubated in
146 cold 4% paraformaldehyde for 3 hours, agitated gently every 30 minutes, then washed with
147 cold PBS for 5 minutes two times. Tissue was stained with Hoescht 33342 (that binds double-
148 stranded DNA) for 30 minutes at room temperature, then hybridised overnight at room
149 temperature with hybridisation buffer (5X SSC, 0.01% SDS, 30% formamide) and 5'-
150 CCATCATCCCCTACTACA-(ATTO 633)-3' oligonucleotide probe specific to '*Ca. Tisiphia*' 16S
151 rRNA (Pilgrim *et al.*, 2017). Hybridised tissue was washed in wash buffer (5X SSC, 0.01% SDS)
152 at 48°C for 60 minutes with gentle shaking every 20 minutes. Samples were then mounted in
153 Vectashield. Images were taken with a ZEIS LSM 880 confocal microscope through ZEIS Zen
154 black, and final images were annotated in Inkscape Ver 1.2 (Inkscape Project, 2020).

155 **De novo sequencing, assembly, and annotation.**

156 A combination of short and long read sequencing was used to construct scaffolds for the '*Ca.*
157 *Tisiphia*' genome. For short reads, Iridian Genomes extracted and processed DNA of one male
158 for Illumina sequencing deposited under bioproject accession PRJNA694375. The short reads
159 of *An. plumbeus* were cleaned with Trimmomatic 0.36 (Bolger, Lohse and Usadel, 2014) and
160 quality checked with FASTQ (Babraham Bioinformatics, 2019). For long reads, genomic DNA
161 from one male was extracted with Qiagen Genomic-tip for ultra-low PacBio sequencing
162 carried out by the Centre for Genomic Research, University of Liverpool. Long read sequences
163 are deposited under bioproject accession number PRJNA901697.

164 A combination of long and short reads were used to assemble as complete a genome for '*Ca.*
165 *Tisiphia*' as possible. First, the '*Ca. Tisiphia*' genome was identified in the Illumina short reads
166 and assembled through Minmap2, MEGAHIT and MetaBAT2 as per the pipeline used in
167 Davison *et al.* (2022). Second, PacBio HiFi long read sequences were assembled using Flye 2.9.
168 1-b1780 with the '-meta' flag to improve sensitivity for low coverage reads. Third, the long
169 read assembly was queried against a local blast database of *Rickettsia* and '*Ca. Tisiphia*'
170 genomes (including the Illumina assembly from the first step) to identify sequences belonging
171 to this strain of '*Ca. Tisiphia*'. Lastly, the long read assembly was polished with the Illumina

172 reads using Polypolish v0.5.0 (Wick and Holt, 2022) with default settings to give 23 final
173 scaffolds.

174 **Phylogeny and metabolic predictions**

175 Annotation of the final assembly was carried out with InterProScan v5 (Jones *et al.*, 2014).
176 Metabolic pathway prediction for presence and completion was carried out through Anvi'o 7
177 using KEGG kofams and COG20 (Aramaki *et al.*, 2020; Eren *et al.*, 2021; Galperin *et al.*, 2021).
178 NRPS pathways were investigated with AntiSMASH 6.0 (Blin *et al.*, 2021).

179 The 'Ca. Tisiphia' strain for *An. plumbeus* was compared to the other existing 'Ca. Tisiphia'
180 genomes through Anvi'o 7. A core genome consisting of 205 gene clusters that contain a total
181 of 3690 genes was found through Anvio-7. Phylogenies were estimated from single copy gene
182 clusters with IQTREE 2.2.0.3 using Model Finder Plus and with 1000 ultrafast bootstraps
183 (Kalyaanamoorthy *et al.*, 2017; Hoang *et al.*, 2018; Minh *et al.*, 2020). The model selected by
184 Model Finder Plus is Q.plant+F+R4. A supporting phylogeny to confirm the identity of 17 kDa
185 OMP genes was produced with the model TIM2+F.

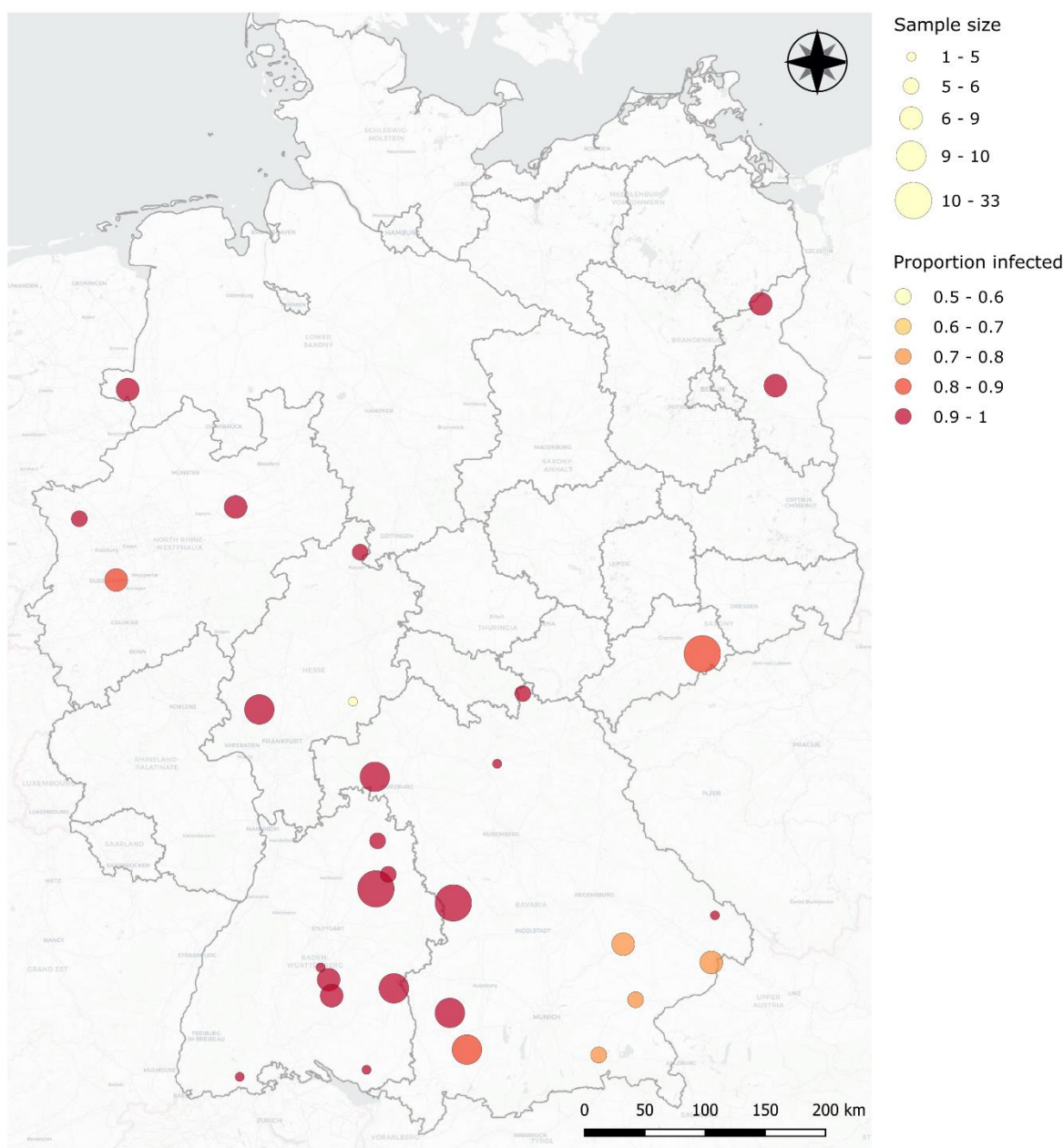
186 **Results and Discussion**

187 **Distribution and predicted environment**

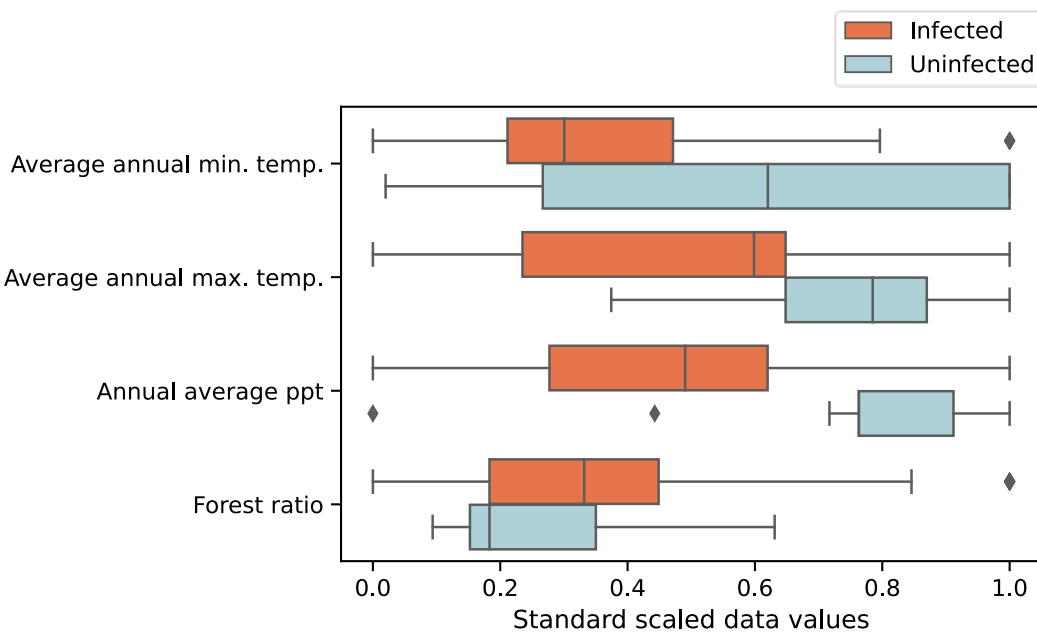
188 'Ca. Tisiphia' was observed to infect *An. plumbeus* across all sites examined in Germany, with
189 95% specimens positive on PCR assay. The few negative specimens were found to mostly
190 occur in the southeast of the country (Figure 1 and Supplementary Figure 1). The infection
191 seems to be stable, and there is no evidence of frequency change over time, with samples
192 from all years spanning 2012 to 2022 displaying similar rates of infection (Supplementary
193 Figure 1, Supplementary Table S1, Supplementary Figure 2).

194 There is no clear evidence of an influence on 'Ca. Tisiphia' infection rates in *An. plumbeus*
195 caused by average minimum or maximum temperature, precipitation or forest types (Figure
196 2 and Supplementary Figure 2 and 3). While there appears to be a significant effect of
197 precipitation on the number of uninfected individuals, this could be an artifact of increased
198 water availability leading to more mosquitoes and thus a higher chance of detecting rarer
199 uninfected individuals (Supplementary Figure 2). No variation is unsurprising as it appears to
200 be a very high prevalence infection. We also acknowledge that using climate databases to
201 retroactively find data is not as accurate as field measurements. However, results agree with

202 previous field observations of *Rickettsia* infection in *Acyrthosiphon pisum* in Japan (Tsuchida
203 *et al.*, 2002). We chose to use the high resolution TerraClim database, but this may still mask
204 small differences in microenvironments are limited to mostly abiotic data. We encourage
205 future symbiosis research to consider environmental measurements to describe the ecology
206 of these organisms more comprehensively.



207 **Figure 1. Map of 'Ca. Tisiphia' infection rates across Germany** where the size of the circle represents the
208 number of individuals sampled and the colour indicates the proportion of 'Ca. Tisiphia' infected individuals.
209 Red = 90-100% infection to light yellow = 50-60% infection. Source data can be found in Supplementary Table
210 S1.



211

212 **Figure 2. Standardised and scaled environmental data** comparing Uninfected (N=13) and Infected (N=237) by
213 environmental variable. Source data can be found in Supplementary Table S1.

214 *Phylogeny and metabolism*

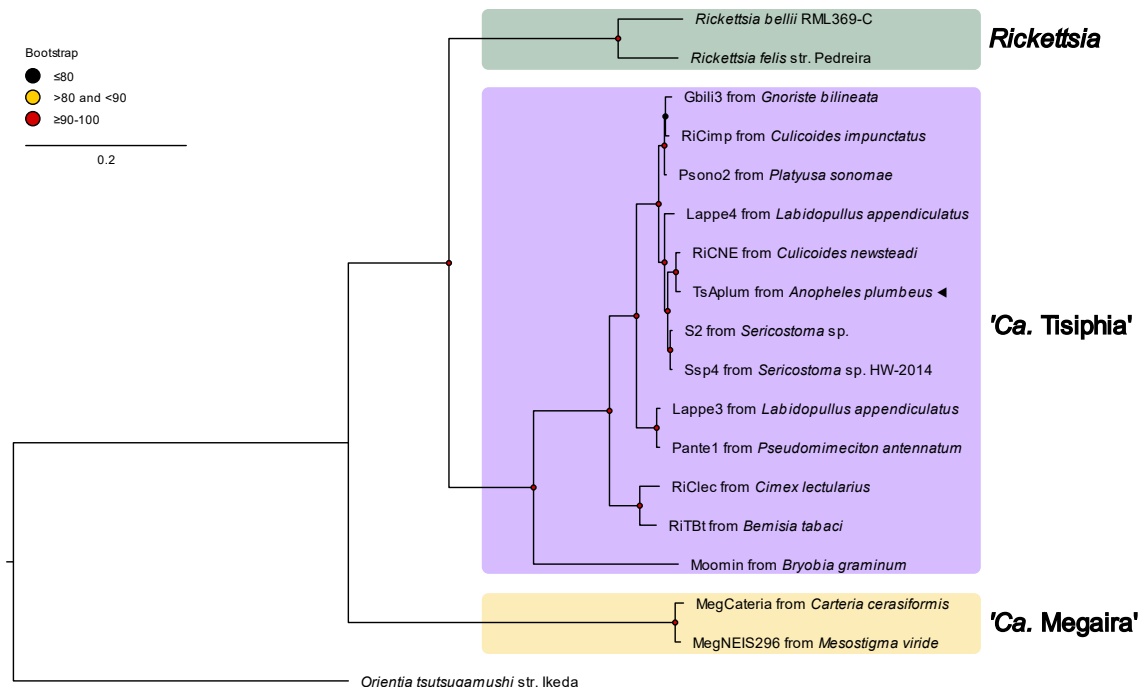
215 The bacteria sequenced from *An. plumbeus* is most closely related to a 'Ca. Tisiphia' found in
216 the biting midge *Culicoides newsteadi* (Figure 3). All infections tested are the same strain of
217 'Ca. Tisiphia' (Supplementary Figure 4). General features of both genomes are consistent with
218 other 'Ca. Tisiphia' (Table 1 and Supplementary Data S2-S4); TsAplum has a single full set of
219 rRNAs (16S, 5S and 23S), and GC content is ~33%. It also has several repeat domains (Table 1)
220 which are associated with protein-protein interactions and are prevalent in *Wolbachia*
221 symbionts (Siozios *et al.*, 2013; Rice, Sheehan and Newton, 2017).

222

223 **Table 1. Summary of the genome assembly for *TsAplum*.**

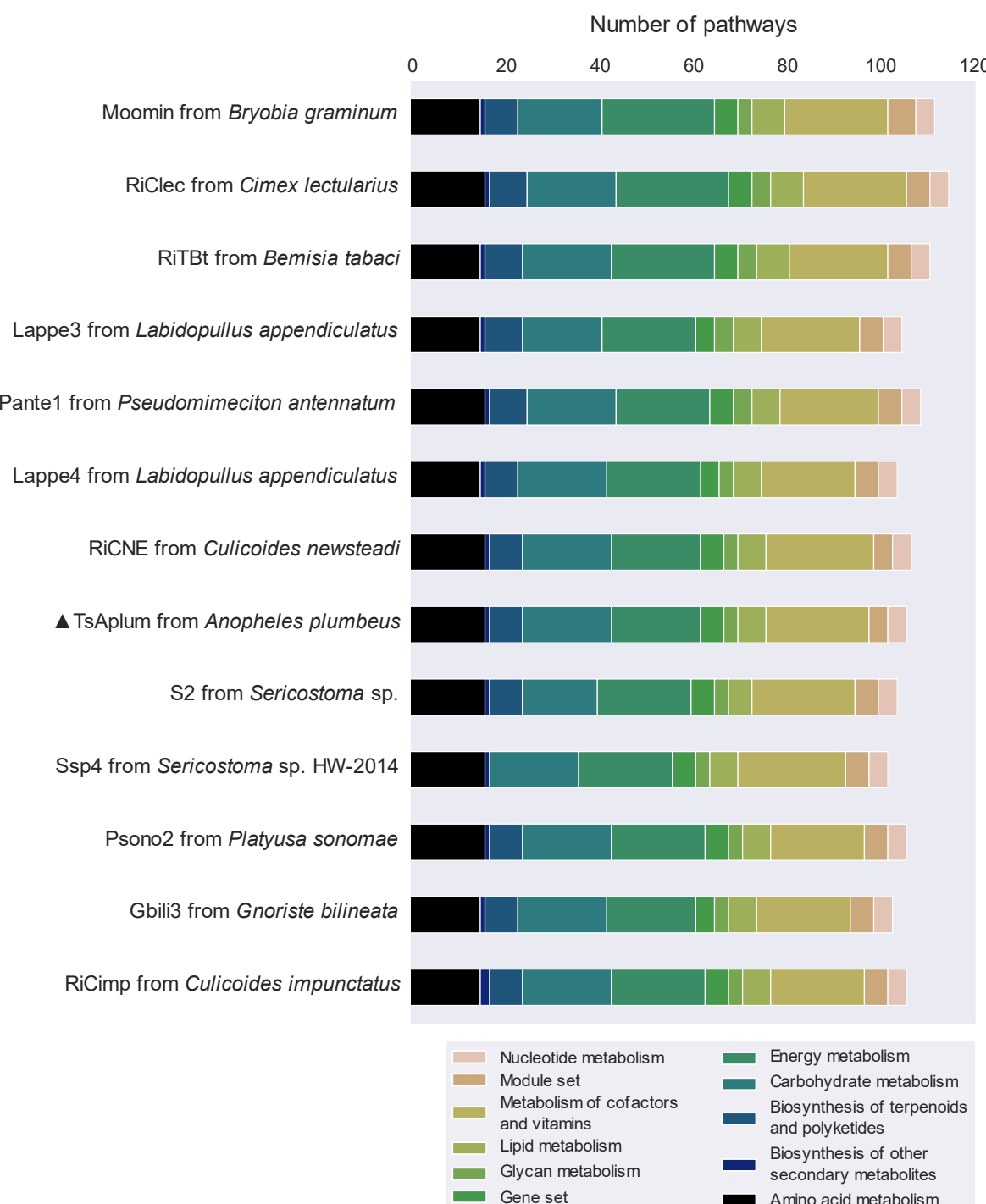
| | | |
|--|--|-----|
| Strain Name | TsAplum | 224 |
| Symbiont genome accession | SAMN31737641 | |
| Host | <i>Anopheles plumbeus</i> | |
| Raw reads accession | Pacbio SRR22298143, Illumina SRR13516402 | |
| Total nucleotides | 1,622,210 | |
| Contigs | 31 | |
| GC content | 32.82% | |
| N50 | 62798 | |
| Number of CDS | 1701 | |
| Avg. CDS length (bp) | 788 | |
| Coding density | 82.57% | |
| rRNAs | 1 x 5S, 1 x 16S, 1 x 23S | |
| tRNAs | 31 | |
| ORFs with Ankyrin repeat domains | 3 | |
| ORFs with Leucine rich repeats | 1 | |
| ORFs with Tetratricopeptide repeats | 6 | |

225

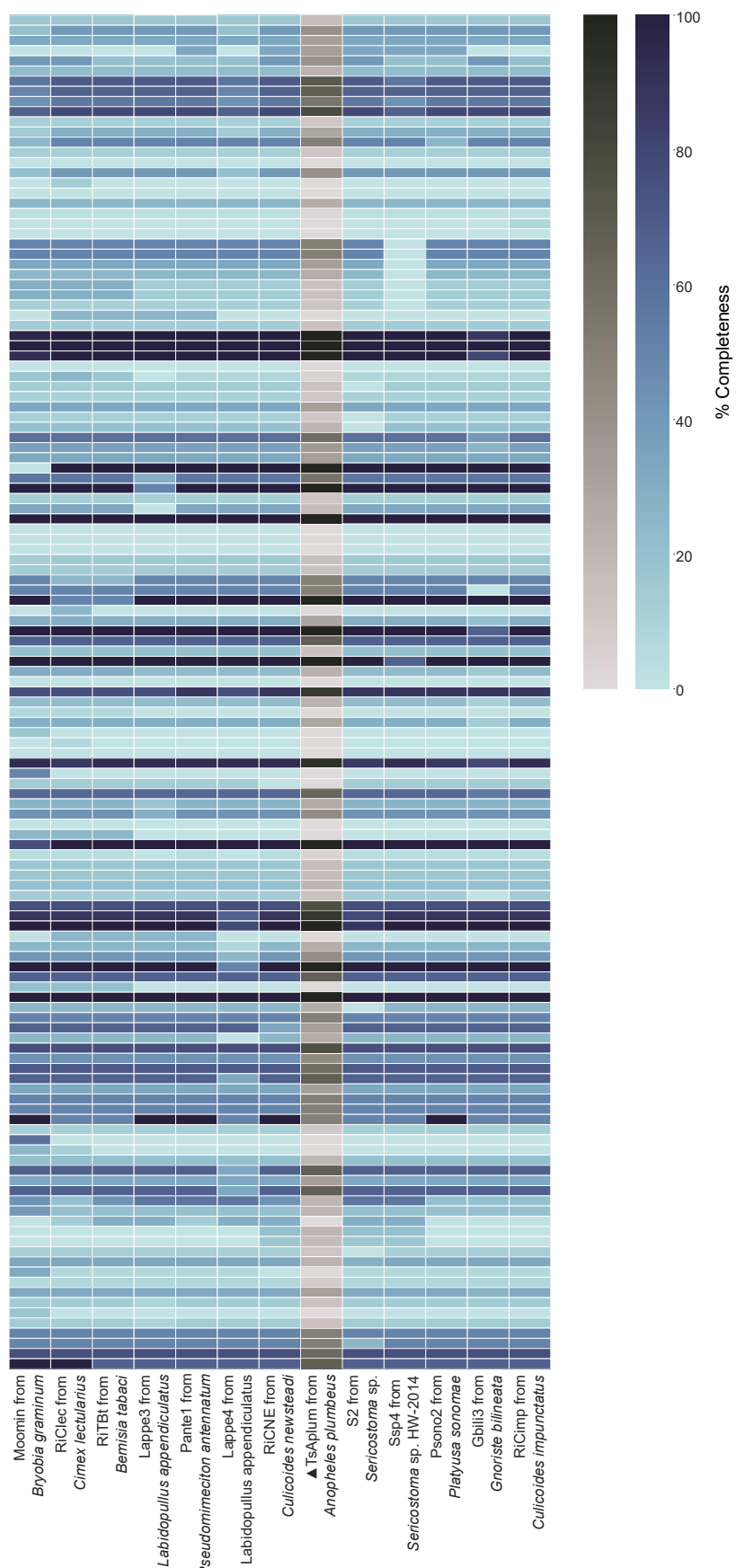


226 **Figure 3. Genome wide phylogeny of 'Ca. Tisiphia' and 'Ca. Megaira'.** Maximum likelihood (ML) phylogeny
227 constructed from 205 single copy gene clusters that contain a total of 3690 genes. New genomes are
228 indicated by ▲ and bootstrap values based on 1000 replicates are indicated with coloured circles (red = 91-
229 100, yellow = 81-90, black <= 80). Accession numbers for each genome are available in Supplementary Table
230 S2.

231 Overall '*Ca. Tisiphia*' found in *An. plumbeus* mirrors the metabolic potential found in other
232 members of its genus (Figure 4 and Figure 5). It does not have any obvious metabolic pathway
233 that would contribute to nutritional symbiosis such as B vitamin production nor any NRPS/PKS
234 system for small molecule synthesis (Supplementary Tables S3 and S4). It does have several
235 toxin/anti-toxin systems as well as secretion pathways Tat, Sec, VirB (Type IV), all of which are
236 essential in various symbiont-host interactions (Masui, Sasaki and Ishikawa, 2000; Meloni *et*
237 *al.*, 2003; Wu *et al.*, 2004; Dale and Moran, 2006; Tseng, Tyler and Setubal, 2009).
238 Additionally, it has a number of ORFs containing ankyrin- and leucine-rich repeats which are
239 thought to be important in interactions with cognate eukaryotic proteins (Siozios *et al.*, 2013;
240 Rice, Sheehan and Newton, 2017). Thus, the genome itself, whilst firmly placing the symbiont
241 in the context of the genus and identifying relatedness to other strains, does not raise obvious
242 hypotheses about the impact of infection on the host. Phenotype studies are required to
243 properly assess the influence of this bacteria on its host. Key studies would address the factors
244 driving the spread of the symbiont into the population (testing for beneficial aspects of
245 infection, cytoplasmic incompatibility, and paternal inheritance) and impacts on viral
246 infection and transmission outcomes.



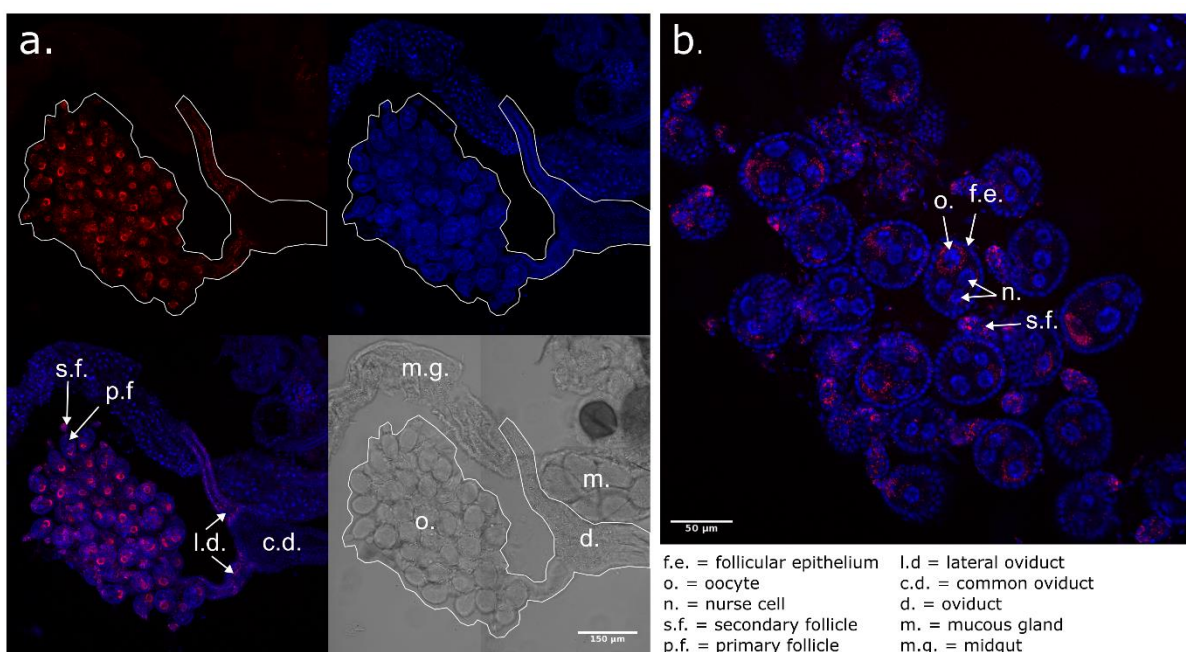
247 **Figure 4. KEGG module distribution in 'Ca. Tisiphia'.** The number of pathways found per genome annotated
248 by KEGG module category for 'Ca. Tisiphia'. Full metadata can be found in Supplementary Data 1. ▲ indicates
249 the genome assembled in this study. Full metadata can be found in Supplementary Tables S3 and S4.



250 **Figure 5. Predicted completeness of KEGG kofam metabolic pathways across 'Ca. Tisiphia'.** The genome
251 assembled in this chapter is coloured grey and indicated with ▲. Full metadata can be found in
252 Supplementary Tables S3 and S4.

253 **FISH imaging**

254 'Ca. Tisiphia' is observed in oocytes and oviduct branches but was not detected in testes
255 (Figure 6 versus Supplementary Figure 5). Localisation and clear polarity of the infection in
256 ovaries strongly suggest that this is a maternally inherited infection (Figure 6). The bacteria
257 cluster around the oocyte of the primary follicles as well as in the lateral ducts and secondary
258 follicles. In *Drosophila melanogaster*, *Wolbachia* is similarly polarised to one end of the
259 primary follicles to the oocyte (Ferree *et al.*, 2005), and in *Proechinophthirus fluctus*, their
260 endosymbionts *Sodalis* appears to use the lateral oviducts to access the ovaries (Boyd *et al.*,
261 2016).



262 **Figure 6. Fluorescence in situ microscopy images of *Anopheles plumbeus* ovaries infected with 'Ca. Tisiphia'.**
263 Red shows 'Ca. Tisiphia' stained with ATTO-633, blue are host nuclei stained with Hoechst. Panels show a) the
264 whole female reproductive organ outlined in white and a breakdown of each light channel and b) a close up of
265 the ovaries showing localised infection within the primary and secondary follicles. White bars indicate a) 150
266 micrometres and b) 50 micrometres.

267 **Final conclusions**

268 *Anopheles plumbeus* and its 'Ca. Tisiphia' make a good potential model for symbioses in
269 *Anopheles* mosquitoes as well as for 'Ca. Tisiphia' infection more generally. Outside of *An.*
270 *plumbeus*, there is only a single well substantiated case of *Wolbachia* and no other symbiont
271 in anopheline mosquitoes (Walker *et al.*, 2021). The infection in *An. plumbeus* is clearly
272 evidenced, likely heritable, and occurs in a species that has seen previous success as a
273 laboratory colony (Kotter, 2005). Beyond this, *An. plumbeus* is a species of interest with the
274 capability to carry West Nile virus and *Plasmodium* parasites (Dekoninck *et al.*, 2011;

275 Schaffner *et al.*, 2012). ‘*Ca. Tisiphia*’ in *An. plumbeus* provides a viable avenue for symbiont-
276 mediated vector modification and control to be tested in anopheline species. It is also an
277 example of a temporally and spatially stable infection of non-pathogenic Rickettsiaceae and
278 a good foil to fluctuating systems like Belli *Rickettsia* in *Bemisia tabaci* (Bockoven *et al.*, 2020).

279 Future work should also establish the effects of this symbiont in transinfection in alternative
280 hosts alongside the native *An. plumbeus* host. Other symbionts like *Wolbachia* are known to
281 produce functionally interesting phenotypes related to vector competence when transferred
282 from the original host into other, naïve species (Moreira *et al.*, 2009). Alongside this, impacts
283 on host function and physiology, and potential means of spread into natural populations
284 would need to be assessed. A first step to establishing transinfection would be to isolate the
285 ‘*Ca. Tisiphia*’ infection into cell culture, which would also represent an important community
286 resource for onward study.

287 In summary, ‘*Ca. Tisiphia*’ is found in 95% of *An. plumbeus* individuals from Germany and
288 forms a well-established, stable, and heritable infection that persists across space and time.
289 Metabolic potential is typical of similar symbiotic bacteria species, and we find no evidence
290 of large-scale environmental factors influencing rates of infection. However, ‘*Ca. Tisiphia*’ and
291 *An. plumbeus* provide a unique opportunity to study the effects of a native symbiont infection
292 in anopheline mosquitoes, as well as explore its potential use for disease mitigation in other
293 species that cannot be infected with currently used symbionts.

294 References

295 Abatzoglou, J.T. *et al.* (2018) 'TerraClimate, a high-resolution global dataset of monthly climate and
296 climatic water balance from 1958–2015', *Scientific Data*, 5(1), p. 170191. Available at:
297 <https://doi.org/10.1038/sdata.2017.191>.

298 Aramaki, T. *et al.* (2020) 'KofamKOALA: KEGG Ortholog assignment based on profile HMM and
299 adaptive score threshold', *Bioinformatics*. Edited by A. Valencia, 36(7), pp. 2251–2252. Available at:
300 <https://doi.org/10.1093/bioinformatics/btz859>.

301 Babraham Bioinformatics (2019) 'Babraham Bioinformatics - FastQC A Quality Control tool for High
302 Throughput Sequence Data'. Babraham Bioinformatics. Available at:
303 <https://www.bioinformatics.babraham.ac.uk/projects/fastqc/> (Accessed: 20 December 2022).

304 Blin, K. *et al.* (2021) 'antiSMASH 6.0: improving cluster detection and comparison capabilities',
305 *Nucleic Acids Research*, 49(W1), pp. W29–W35. Available at: <https://doi.org/10.1093/nar/gkab335>.

306 Bockoven, A.A. *et al.* (2020) 'What goes up might come down: the spectacular spread of an
307 endosymbiont is followed by its decline a decade later', *Microbial Ecology*, 79(2), pp. 482–494.
308 Available at: <https://doi.org/10.1007/s00248-019-01417-4>.

309 Bodnar, J.L. *et al.* (2018) 'The folA gene from the *Rickettsia* endosymbiont of *Ixodes pacificus*
310 encodes a functional dihydrofolate reductase enzyme', *Ticks and Tick-borne Diseases*, 9(3), pp. 443–
311 449. Available at: <https://doi.org/10.1016/j.ttbdis.2017.12.013>.

312 Bolger, A.M., Lohse, M. and Usadel, B. (2014) 'Trimmomatic: a flexible trimmer for Illumina sequence
313 data', *Bioinformatics (Oxford, England)*, 30(15), pp. 2114–2120. Available at:
314 <https://doi.org/10.1093/bioinformatics/btu170>.

315 Boyd, B.M. *et al.* (2016) 'Two bacterial genera, *Sodalis* and *Rickettsia*, associated with the seal louse
316 *Proechinophthirus fluctus* (Phthiraptera: Anoplura)', *Applied and Environmental Microbiology*,
317 82(11), pp. 3185–3197. Available at: [https://doi.org/10.1128/AEM.00282-16/SUPPL_FILE/ZAM999117155SO1.PDF](https://doi.org/10.1128/AEM.00282-16).

319 Buchner, P. (1965) *Endosymbiosis of animals with plant microorganisms*. New York: Interscience
320 Publishers.

321 Bueno-Marí, R. and Jiménez-Peydró, R. (2011) 'Anopheles plumbeus Stephens, 1828: a neglected
322 malaria vector in Europe', *Malaria Reports*, 1(1), p. 2. Available at:
323 <https://doi.org/10.4081/malaria.2011.e2>.

324 Cass, B.N. *et al.* (2016) 'Conditional fitness benefits of the *Rickettsia* bacterial symbiont in an insect
325 pest', *Oecologia*, 180(1), pp. 169–179. Available at: <https://doi.org/10.1007/s00442-015-3436-x>.

326 Corbin, C. *et al.* (2017) 'Heritable symbionts in a world of varying temperature', *Heredity*, 118(1), pp.
327 10–20. Available at: <https://doi.org/10.1038/hdy.2016.71>.

328 Dale, C. and Moran, N.A. (2006) 'Molecular Interactions between Bacterial Symbionts and Their
329 Hosts', *Cell*, 126(3), pp. 453–465. Available at: <https://doi.org/10.1016/j.cell.2006.07.014>.

330 Dekoninck, W. *et al.* (2011) 'Human-Induced Expanded Distribution of *Anopheles plumbeus*,
331 Experimental Vector of West Nile Virus and a Potential Vector of Human Malaria in Belgium', *Journal
332 of Medical Entomology*, 48(4), pp. 924–928. Available at: <https://doi.org/10.1603/ME10235>.

333 Driscoll, T. *et al.* (2013) 'Bacterial DNA sifted from the *Trichoplax adhaerens* (Animalia: Placozoa)
334 genome project reveals a putative rickettsial endosymbiont', *Genome Biology and Evolution*, 5(4),
335 pp. 621–645. Available at: <https://doi.org/10.1093/GBE/EVT036>.

336 Dunbar, H.E. *et al.* (2007) 'Aphid thermal tolerance is governed by a point mutation in bacterial
337 symbionts', *PLoS Biology*, 5(5), pp. 1006–1015. Available at:
338 <https://doi.org/10.1371/journal.pbio.0050096>.

339 Dyková, I. *et al.* (2013) 'Nuclearia pattersoni sp. n. (Filosea), a new species of amphizoic amoeba
340 isolated from gills of roach (*Rutilus rutilus*), and its rickettsial endosymbiont', *Folia Parasitologica*,
341 50(3), pp. 161–170. Available at: <https://doi.org/10.14411/fp.2003.030>.

342 Eren, A.M. *et al.* (2021) 'Community-led, integrated, reproducible multi-omics with anvi'o', *Nature
343 Microbiology*, 6(1), pp. 3–6. Available at: <https://doi.org/10.1038/s41564-020-00834-3>.

344 European Union (2018) *Copernicus Land Monitoring Service*, European Environment Agency (EEA).
345 Available at: <https://land.copernicus.eu/pan-european/high-resolution-layers/forests/forest-type-1/status-maps/forest-type-2018> (Accessed: 31 August 2022).

347 Ferree, P.M. *et al.* (2005) 'Wolbachia Utilizes Host Microtubules and Dynein for Anterior Localization
348 in the *Drosophila* Oocyte', *PLOS Pathogens*, 1(2), p. e14. Available at:
349 <https://doi.org/10.1371/journal.ppat.0010014>.

350 Folmer, O. *et al.* (1994) 'DNA primers for amplification of mitochondrial cytochrome c oxidase
351 subunit I from diverse metazoan invertebrates', *Molecular Marine Biology and Biotechnology*, 3(5),
352 pp. 294–299.

353 Galperin, M.Y. *et al.* (2021) 'COG database update: focus on microbial diversity, model organisms,
354 and widespread pathogens', *Nucleic Acids Research*, 49(D1), pp. D274–D281. Available at:
355 <https://doi.org/10.1093/nar/gkaa1018>.

356 Giorgini, M. *et al.* (2010) 'Rickettsia symbionts cause parthenogenetic reproduction in the parasitoid
357 wasp *Pnigalio soemius* (hymenoptera: Eulophidae)', *Applied and Environmental Microbiology*, 76(8),
358 pp. 2589–2599. Available at: <https://doi.org/10.1128/AEM.03154-09>.

359 Hajibabaei, M. *et al.* (2005) 'Critical factors for assembling a high volume of DNA barcodes',
360 *Philosophical Transactions of the Royal Society B: Biological Sciences*, 360(1462), pp. 1959–1967.
361 Available at: <https://doi.org/10.1098/rstb.2005.1727>.

362 Hayashi, M. *et al.* (2016) 'A Nightmare for Males? A Maternally Transmitted Male-Killing Bacterium
363 and Strong Female Bias in a Green Lacewing Population', *PLOS ONE*. Edited by K. Bourtzis, 11(6), p.
364 e0155794. Available at: <https://doi.org/10.1371/journal.pone.0155794>.

365 Hendry, T.A., Hunter, M.S. and Baltrus, D.A. (2014) 'The facultative symbiont *Rickettsia* protects an
366 invasive whitefly against entomopathogenic *Pseudomonas syringae* strains', *Applied and
367 Environmental Microbiology*, 80(23), pp. 7161–7168. Available at:
368 <https://doi.org/10.1128/AEM.02447-14>.

369 Heym, E.C. *et al.* (2017) 'Anopheles plumbeus (Diptera: Culicidae) in Germany: updated geographic
370 distribution and public health impact of a nuisance and vector mosquito', *Tropical Medicine &
371 International Health*, 22(1), pp. 103–112. Available at: <https://doi.org/10.1111/tmi.12805>.

372 Himler, A.G. *et al.* (2011) 'Rapid Spread of a Bacterial Symbiont in an Invasive Whitefly Is Driven by
373 Fitness Benefits and Female Bias', *Science*, 332(6026), pp. 254–256. Available at:
374 <https://doi.org/10.1126/science.1199410>.

375 Hoang, D.T. *et al.* (2018) 'UFBoot2: Improving the Ultrafast Bootstrap approximation', *Molecular
376 Biology and Evolution*, 35(2), pp. 518–522. Available at: <https://doi.org/10.5281/zenodo.854445>.

377 Hoffmann, A.A. *et al.* (2011) 'Successful establishment of Wolbachia in Aedes populations to
378 suppress dengue transmission', *Nature*, 476(7361), pp. 454–457. Available at:
379 <https://doi.org/10.1038/nature10356>.

380 Hollants, J. *et al.* (2013) 'Permanent residents or temporary lodgers: Characterizing intracellular
381 bacterial communities in the siphonous green alga *bryopsis*', *Proceedings of the Royal Society B:
382 Biological Sciences*, 280(1754), pp. 1–8. Available at: <https://doi.org/10.1098/rspb.2012.2659>.

383 Hughes, G.L. *et al.* (2014) 'Native microbiome impedes vertical transmission of *Wolbachia* in
384 *Anopheles* mosquitoes', *Proceedings of the National Academy of Sciences*, 111(34), pp. 12498–
385 12503. Available at: <https://doi.org/10.1073/pnas.1408888111>.

386 Hunter, J.D. (2007) 'Matplotlib: A 2D Graphics Environment', *Computing in Science & Engineering*,
387 9(3), pp. 90–95. Available at: <https://doi.org/10.1109/MCSE.2007.55>.

388 Hurst, G.D.D. *et al.* (1994) 'The effect of infection with male-killing *Rickettsia* on the demography of
389 female *Adalia bipunctata* L. (two spot ladybird)', *Heredity*, 73(3), pp. 309–316. Available at:
390 <https://doi.org/10.1038/hdy.1994.138>.

391 Inkscape Project (2020) 'Inkscape'. Available at: <https://inkscape.org>.

392 Jones, P. *et al.* (2014) 'InterProScan 5: genome-scale protein function classification', *Bioinformatics*,
393 30(9), pp. 1236–1240. Available at: <https://doi.org/10.1093/bioinformatics/btu031>.

394 Kalyaanamoorthy, S. *et al.* (2017) 'ModelFinder: Fast model selection for accurate phylogenetic
395 estimates', *Nature Methods*, 14(6), pp. 587–589. Available at: <https://doi.org/10.1038/nmeth.4285>.

396 Kang, Y.J. *et al.* (2014) 'Extensive diversity of *Rickettsiales* bacteria in two species of ticks from China
397 and the evolution of the *Rickettsiales*', *BMC Evolutionary Biology*, 14(1), pp. 1–12. Available at:
398 <https://doi.org/10.1186/S12862-014-0167-2/FIGURES/4>.

399 Kikuchi, Y. and Fukatsu, T. (2005) 'Rickettsia Infection in Natural Leech Populations', *Microbial
400 Ecology*, 49(2), pp. 265–271. Available at: <https://doi.org/10.1007/s00248-004-0140-5>.

401 Kotter, H. (2005) *Bionomie und Verbreitung der autochthonen Fiebermücke Anopheles plumbeus
402 (Culicidae) und ihrer Vektorkompetenz für Plasmodium falciparum, Erreger der Malaria tropica*.
403 Available at: <https://doi.org/10.11588/heidok.00006104>.

404 Kremer, N. *et al.* (2009) 'Wolbachia Interferes with Ferritin Expression and Iron Metabolism in
405 Insects', *PLoS Pathogens*, 5(10), p. e1000630. Available at:
406 <https://doi.org/10.1371/journal.ppat.1000630>.

407 Leclair, M. *et al.* (2017) 'Consequences of coinfection with protective symbionts on the host
408 phenotype and symbiont titres in the pea aphid system', *Insect Science*, 24(5), pp. 798–808.
409 Available at: <https://doi.org/10.1111/1744-7917.12380>.

410 Masui, S., Sasaki, T. and Ishikawa, H. (2000) 'Genes for the Type IV Secretion System in an
411 Intracellular Symbiont, Wolbachia, a Causative Agent of Various Sexual Alterations in Arthropods',
412 *Journal of Bacteriology*, 182(22), pp. 6529–6531.

413 Meloni, S. *et al.* (2003) 'The twin-arginine translocation (Tat) system is essential for Rhizobium–
414 legume symbiosis', *Molecular Microbiology*, 48(5), pp. 1195–1207. Available at:
415 <https://doi.org/10.1046/j.1365-2958.2003.03510.x>.

416 Minh, B.Q. *et al.* (2020) 'IQ-TREE 2: New models and efficient methods for phylogenetic inference in
417 the genomic era', *Molecular Biology and Evolution*. Edited by E. Teeling, 37(5), pp. 1530–1534.
418 Available at: <https://doi.org/10.1093/molbev/msaa015>.

419 Moran, N.A., McCutcheon, J.P. and Nakabachi, A. (2008) 'Genomics and Evolution of Heritable
420 Bacterial Symbionts', *Annual Review of Genetics*, 42(1), pp. 165–190. Available at:
421 <https://doi.org/10.1146/annurev.genet.41.110306.130119>.

422 Moreira, L.A. *et al.* (2009) 'A Wolbachia Symbiont in Aedes aegypti Limits Infection with Dengue,
423 Chikungunya, and Plasmodium', *Cell*, 139(7), pp. 1268–1278. Available at:
424 <https://doi.org/10.1016/j.cell.2009.11.042>.

425 Pedregosa, F. *et al.* (2011) 'Scikit-learn: Machine Learning in Python', *Journal of Machine Learning
426 Research*, 12(85), pp. 2825–2830.

427 Pereira, T.N. *et al.* (2018) 'Wolbachia significantly impacts the vector competence of Aedes aegypti
428 for Mayaro virus', *Scientific Reports*, 8(1), pp. 1–9. Available at: [https://doi.org/10.1038/s41598-018-25236-8](https://doi.org/10.1038/s41598-018-
429 25236-8).

430 Pilgrim, J. *et al.* (2017) 'Torix group *Rickettsia* are widespread in Culicoides biting midges (Diptera:
431 Ceratopogonidae), reach high frequency and carry unique genomic features', *Environmental
432 Microbiology*, 19(10), pp. 4238–4255. Available at: <https://doi.org/10.1111/1462-2920.13887>.

433 Pilgrim, J. *et al.* (2021) 'Torix *Rickettsia* are widespread in arthropods and reflect a neglected
434 symbiosis', *GigaScience*, 10(3), pp. 1–19. Available at: <https://doi.org/10.1093/gigascience/giab021>.

435 QGIS.org (2020) 'QGIS 3.16'. Hannover: QGIS Association. Available at: <http://www.qgis.org/>.

436 Rice, D.W., Sheehan, K.B. and Newton, I.L.G. (2017) 'Large-Scale Identification of *Wolbachia pipiensis*
437 Effectors', *Genome Biology and Evolution*, 9(7), pp. 1925–1937. Available at:
438 <https://doi.org/10.1093/gbe/evx139>.

439 Rossum, G.V. and Drake, F.L. (2009) *Python 3 Reference Manual*. Scotts Valley, CA: CreateSpace.

440 Schaffner, F. *et al.* (2012) 'Anopheles plumbeus (Diptera: Culicidae) in Europe: A mere nuisance
441 mosquito or potential malaria vector?', *Malaria Journal*, 11, p. 393. Available at:
442 <https://doi.org/10.1186/1475-2875-11-393>.

443 Schrallhammer, M. *et al.* (2013) "Candidatus Megaira polyxenophila" gen. nov., sp. nov.:
444 Considerations on Evolutionary History, Host Range and Shift of Early Divergent *Rickettsiae*', *PLoS
445 ONE*. Edited by S.A. Ralph, 8(8), p. e72581. Available at:
446 <https://doi.org/10.1371/journal.pone.0072581>.

447 Seabold, S. and Perktold, J. (2010) 'Statsmodels: Econometric and Statistical Modeling with Python',
448 *PROC. OF THE 9th PYTHON IN SCIENCE CONF.* Available at: <http://statsmodels.sourceforge.net/>
449 (Accessed: 11 February 2021).

450 Siozios, S. *et al.* (2013) 'The diversity and evolution of *Wolbachia* ankyrin repeat domain genes', *PLoS ONE*, 8(2), p. e55390. Available at: <https://doi.org/10.1371/journal.pone.0055390>.

452 Siozios, S. *et al.* (2020) 'DNA barcoding reveals incorrect labelling of insects sold as food in the UK',
453 *PeerJ*, 8, p. e8496. Available at: <https://doi.org/10.7717/peerj.8496>.

454 Thongprem, P. *et al.* (2020) 'Transmission, tropism, and biological impacts of torix *Rickettsia* in the
455 common bed bug *Cimex lectularius* (Hemiptera: Cimicidae)', *Frontiers in Microbiology*, 11. Available
456 at: <https://doi.org/10.3389/fmicb.2020.608763>.

457 Tseng, T.-T., Tyler, B.M. and Setubal, J.C. (2009) 'Protein secretion systems in bacterial-host
458 associations, and their description in the Gene Ontology', *BMC Microbiology*, 9(1), p. S2. Available at:
459 <https://doi.org/10.1186/1471-2180-9-S1-S2>.

460 Tsuchida, T. *et al.* (2002) 'Diversity and geographic distribution of secondary endosymbiotic bacteria
461 in natural populations of the pea aphid, *Acyrthosiphon pisum*', *Molecular Ecology*, 11(10), pp. 2123–
462 2135. Available at: <https://doi.org/10.1046/j.1365-294X.2002.01606.x>.

463 Vega, I.A., Arribére, M.A. and Castro-Vazquez, A. (2012) 'Apple snails and their endosymbionts
464 bioconcentrate heavy metals and uranium from contaminated drinking water', *Environmental
465 Science and Pollution Research*, 19, pp. 3307–3316. Available at: <https://doi.org/10.1007/s11356-012-0848-6>.

467 Walker, T. *et al.* (2011) 'The wMel Wolbachia strain blocks dengue and invades caged *Aedes aegypti*
468 populations', *Nature*, 476(7361), pp. 450–453. Available at: <https://doi.org/10.1038/nature10355>.

469 Walker, T. *et al.* (2021) 'Stable high-density and maternally inherited Wolbachia infections in
470 *Anopheles moucheti* and *Anopheles demeilloni* mosquitoes', *Current Biology*, 31(11), pp. 2310–
471 2320.e5. Available at: <https://doi.org/10.1016/j.cub.2021.03.056>.

472 Waskom, M. and Seaborn development team (2020) 'mwaskom/seaborn'. Zenodo. Available at:
473 <https://doi.org/10.5281/zenodo.592845>.

474 Werner, D. *et al.* (2014) 'The citizen science project "Mückenatlas" supports mosquito (Diptera,
475 Culicidae) monitoring in Germany.', *Proceedings of the 8th International Conference on Urban Pests,
476 20-23 July 2014, Zurich, Switzerland*, pp. 119–124.

477 Wick, R.R. and Holt, K.E. (2022) 'Polypolish: Short-read polishing of long-read bacterial genome
478 assemblies', *PLoS computational biology*, 18(1), p. e1009802. Available at:
479 <https://doi.org/10.1371/journal.pcbi.1009802>.

480 Wu, M. *et al.* (2004) 'Phylogenomics of the Reproductive Parasite *Wolbachia* *pipiensis* wMel: A
481 Streamlined Genome Overrun by Mobile Genetic Elements', *PLoS Biology*, 2(3), p. e69. Available at:
482 <https://doi.org/10.1371/journal.pbio.0020069>.

483 Xie, J. *et al.* (2014) 'Male killing Spiroplasma protects *Drosophila melanogaster* against two
484 parasitoid wasps', *Heredity*, 112(4), pp. 399–408. Available at:
485 <https://doi.org/10.1038/hdy.2013.118>.

486 Zchori-Fein, E., Borad, C. and Harari, A.R. (2006) 'Oogenesis in the date stone beetle, *Coccotrypes*
487 *dactyliperda*, depends on symbiotic bacteria', *Physiological Entomology*, 31(2), pp. 164–169.
488 Available at: <https://doi.org/10.1111/j.1365-3032.2006.00504.x>.

489

490 **Table and Figure legends**

491 **Figure 1. Map of 'Ca. Tisiphia' infection rates across Germany** where the size of the circle
492 represents the number of individuals sampled and the colour indicates the proportion of
493 'Ca. Tisiphia' infected individuals. Red = 90-100% infection to light yellow = 50-60%
494 infection. Source data can be found in Supplementary Table S1.

495 **Figure 2. Standardised and scaled environmental data** comparing Uninfected (N=13) and
496 Infected (N=237) by environmental variable. Source data can be found in Supplementary
497 Table S1.

498 **Figure 3. Genome wide phylogeny of 'Ca. Tisiphia' and 'Ca. Megaira'.** Maximum likelihood
499 (ML) phylogeny constructed from 205 single copy gene clusters that contain a total of 3690
500 genes. New genomes are indicated by ◀ and bootstrap values based on 1000 replicates are
501 indicated with coloured circles (red = 91-100, yellow = 81-90, black <= 80). Accession
502 numbers for each genome are available in Supplementary Table S2.

503 **Figure 4. KEGG module distribution in 'Ca. Tisiphia'.** The number of pathways found per
504 genome annotated by KEGG module category for 'Ca. Tisiphia'. Full metadata can be found
505 in Supplementary data. ▲ indicates the genome assembled in this study. Full metadata can
506 be found in Supplementary Tables S3 and S4.

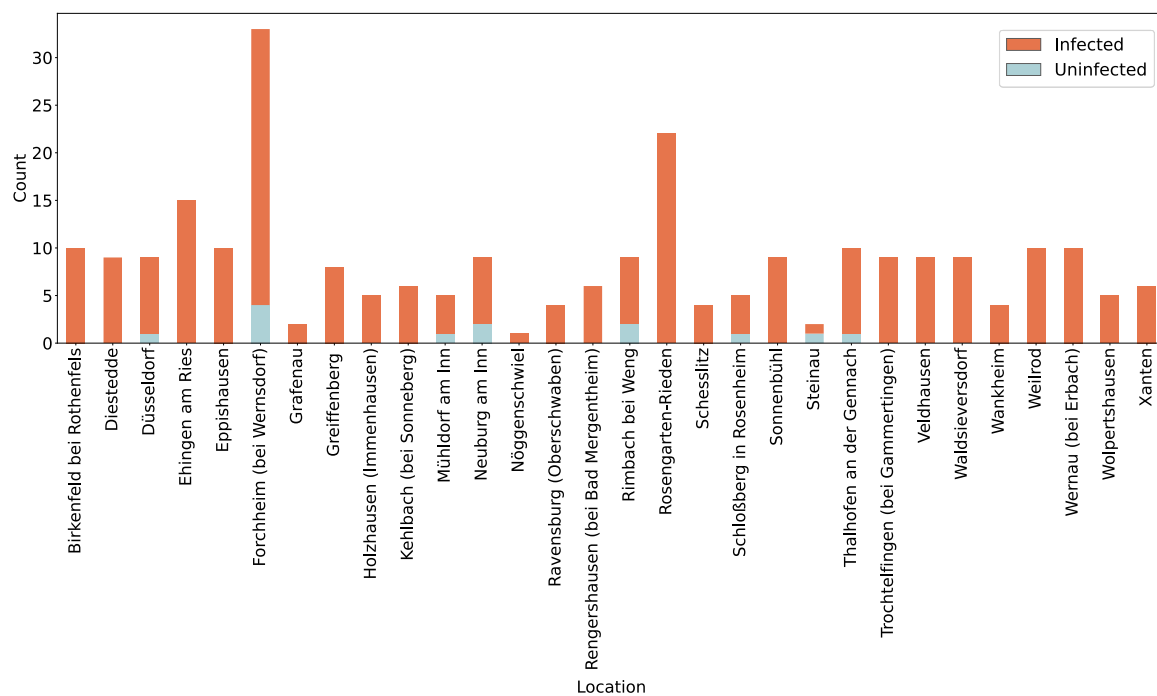
507 **Figure 5. Predicted completeness of KEGG kofam metabolic pathways across 'Ca. Tisiphia'.**
508 The genome assembled in this chapter is coloured grey and indicated with ▲. Full metadata
509 can be found in Supplementary Tables S3 and S4.

510 **Figure 6. Fluorescence in situ microscopy images of *Anopheles plumbeus* ovaries infected
511 with 'Ca. Tisiphia'.** Red shows 'Ca. Tisiphia' stained with ATTO-633, blue are host nuclei
512 stained with Hoechst. Panels show a) the whole female reproductive organ outlined in white
513 and a breakdown of each light channel and b) a close up of the ovaries showing localised
514 infection within the primary and secondary follicles. White bars indicate a) 150 micrometres
515 and b) 50 micrometres.

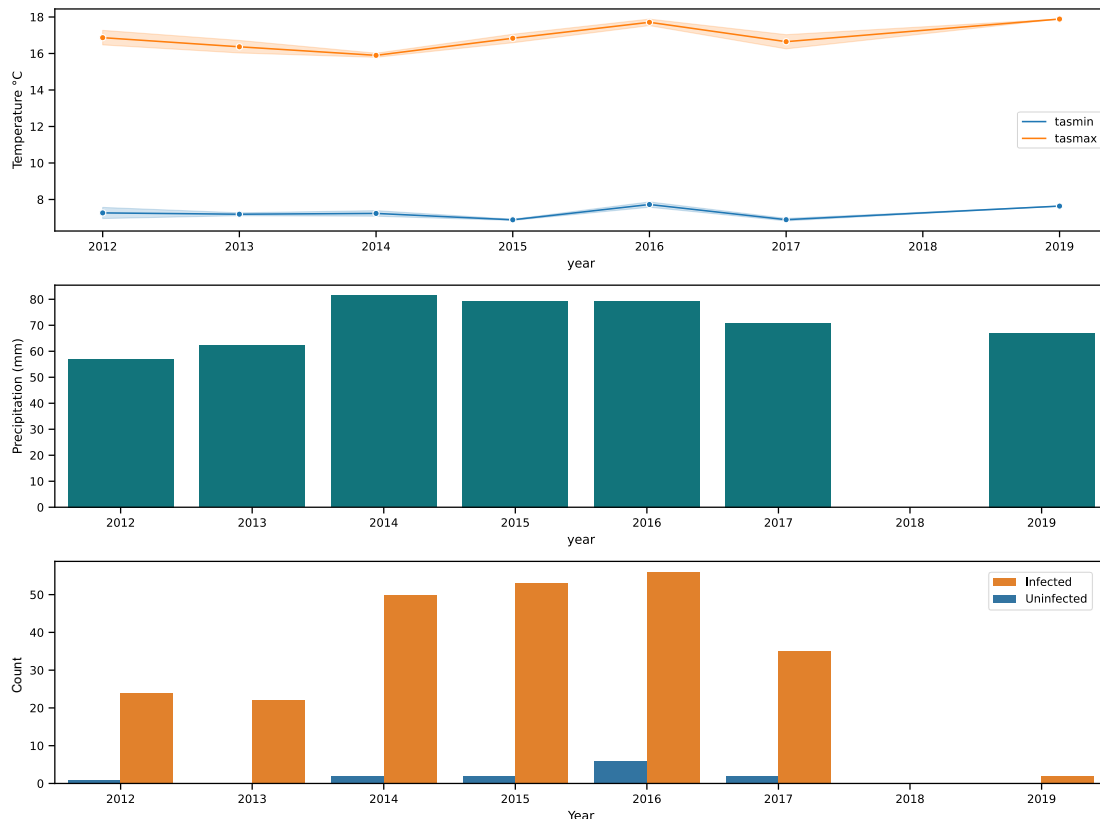
516 **Figure 7. Fluorescence in situ microscopy images of *Anopheles plumbeus* testes.** Blue are
517 host nuclei stained with Hoechst 33342, Red is ATTO-633 auto-fluorescence in the testes not
518 'Ca. Tisiphia' staining. White bars indicate a) 150 micrometres and b) 50 micrometres.

519 **Table 1. Summary of the genome assembly for TsAplum.**

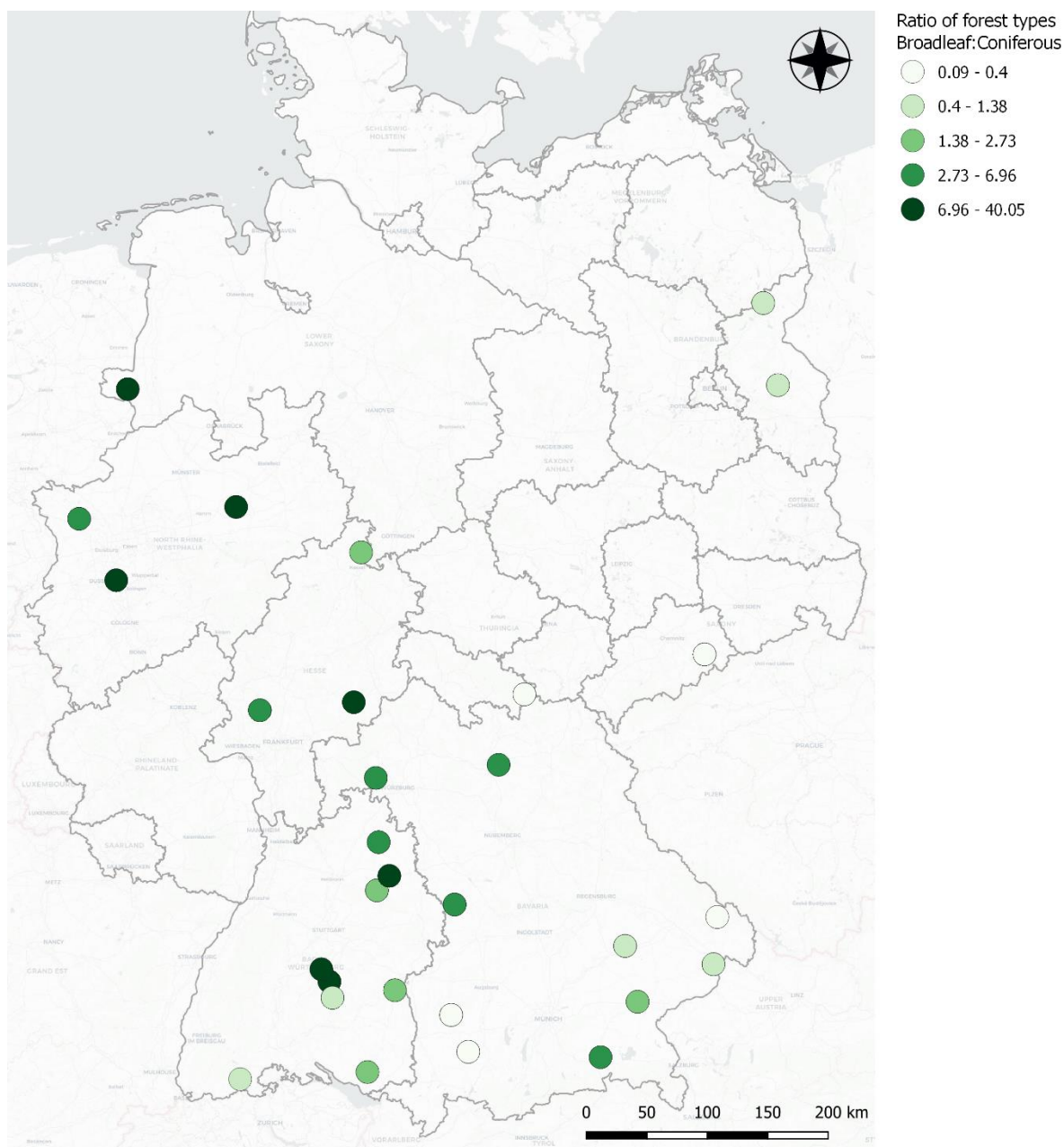
520 **Supplementary Figures**



521 **Supplementary Figure 1. 'Ca. Tisiphia' infection rates by site**. Infected samples are shown in orange, 522 uninfected are shown in light blue. Source data can be found in Supplementary Table S1.



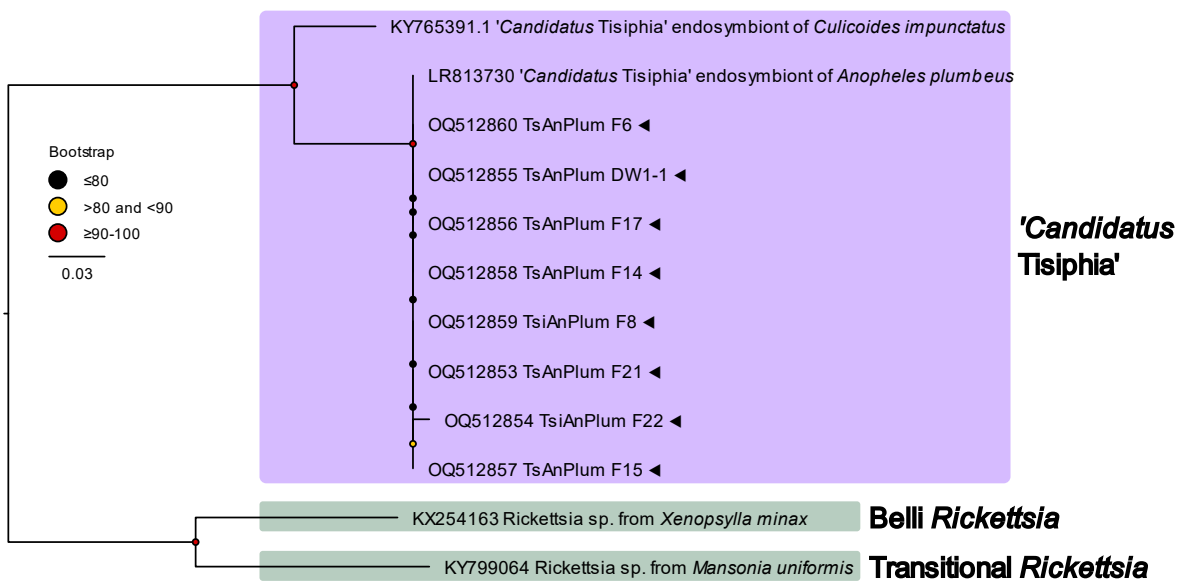
523 **Supplementary Figure 2. Environmental data for *Anopheles plumbeus* collection sites across Germany**
 524 **extracted from the TerraClim database**. (Top) average annual minimum and maximum temperature across all
 525 *An. plumbeus* collection sites in Germany. (Middle) average annual precipitation across all sites. (Bottom)
 526 counts of infected and uninfected individuals across all sites where dark blue = infected and orange =
 527 uninfected.
 528



529

530 **Supplementary Figure 3. The ratio of broadleaf to coniferous forest in a 3km radius of each collection site.**
531 Darker green indicates more broadleaf, lighter green indicates closer to equal proportions. Source data can be
532 found in Supplementary Table S1.

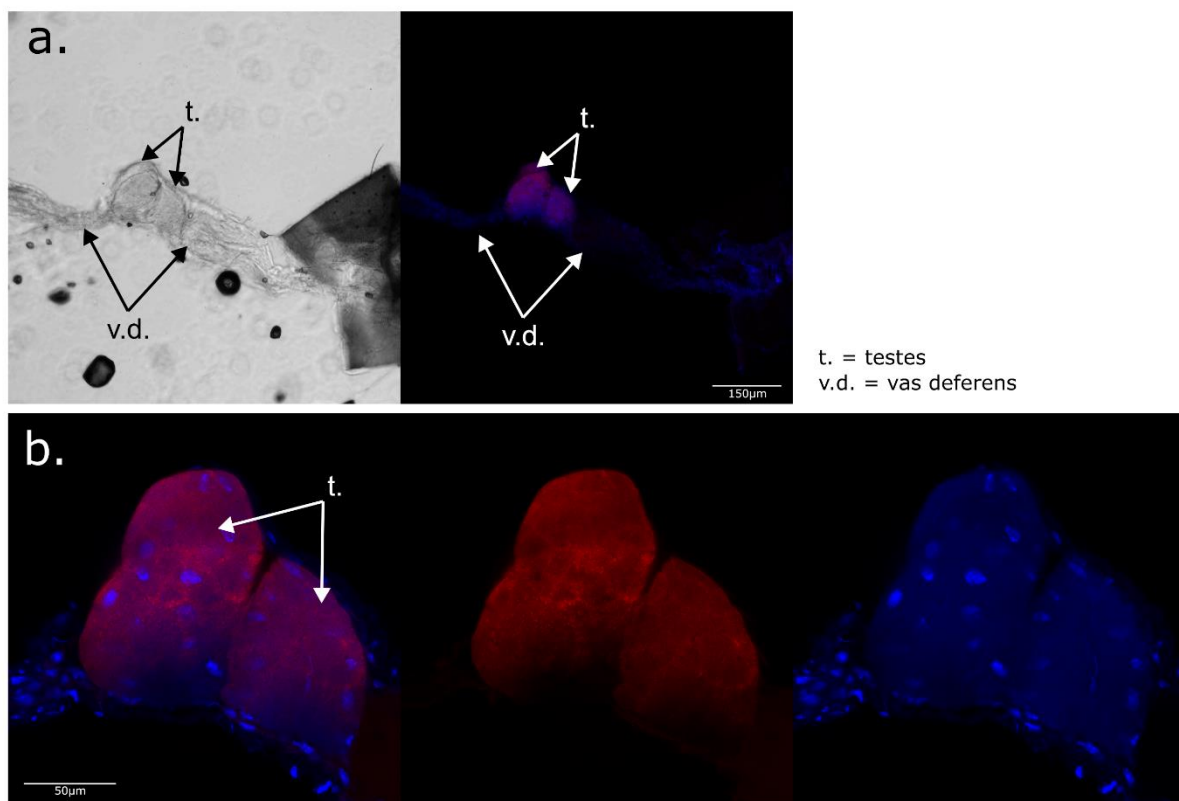
533



534

535 **Supplementary Figure 4. Maximum likelihood tree for 17 kDa surface antigen (omp) for 'Candidatus**
 536 **Tisiphia'** extracted from *An. plumbeus*. New genomes are indicated by ▲ and bootstrap values based on
 537 1000 replicates are indicated with coloured circles (red = 91-100, yellow = 81-90, black <= 80).

538



539 **Supplementary Figure 5. Fluorescence in situ microscopy images of *Anopheles plumbeus* testes.** Blue are
540 host nuclei stained with Hoechst 33342, Red is ATTO-633 auto-fluorescence in the testes not 'Ca. Tisiphia'
541 staining. White bars indicate a) 150 micrometres and b) 50 micrometres.